


# Value of T<sub>2</sub> Mapping MRI for Prostate Cancer Detection and Classification

Maximilian Klingebiel, MD,<sup>1</sup> Lars Schimmöller, MD,<sup>1\*</sup>  Elisabeth Weiland, PhD,<sup>2</sup> Tobias Franiel, MD,<sup>3</sup> Kai Jannusch, MD,<sup>1</sup> Julian Kirchner, MD,<sup>1</sup> Tom Hilbert,<sup>4,5,6</sup> Ralph Strecker,<sup>7</sup> Christian Arsov, MD,<sup>8</sup> Hans-Jörg Wittsack, PhD,<sup>1</sup> Peter Albers, MD,<sup>8</sup> Gerald Antoch, MD,<sup>1</sup> and Tim Ullrich, MD<sup>1</sup>

**Background:** Currently, multi-parametric prostate MRI (mpMRI) consists of a qualitative T<sub>2</sub>, diffusion weighted, and dynamic contrast enhanced imaging. Quantification of T<sub>2</sub> imaging might further standardize PCa detection and support artificial intelligence solutions.

**Purpose:** To evaluate the value of T<sub>2</sub> mapping to detect prostate cancer (PCa) and to differentiate PCa aggressiveness.

**Study Type:** Retrospective single center cohort study.

**Population:** Forty-four consecutive patients (mean age 67 years; median PSA 7.9 ng/mL) with mpMRI and verified PCa by subsequent targeted plus systematic MR/ultrasound (US)-fusion biopsy from February 2019 to December 2019.

**Field Strength/Sequence:** Standardized mpMRI at 3 T with an additionally acquired T<sub>2</sub> mapping sequence.

**Assessment:** Primary endpoint was the analysis of quantitative T<sub>2</sub> values and contrast differences/ratios (CD/CR) between PCa and benign tissue. Secondary objectives were the correlation between T<sub>2</sub> values, ISUP grade, apparent diffusion coefficient (ADC) value, and PI-RADS, and the evaluation of thresholds for differentiating PCa and clinically significant PCa (csPCa).

**Statistical Tests:** Mann–Whitney test, Spearman's rank ( $r_s$ ) correlation, receiver operating curves, Youden's index (J), and AUC were performed. Statistical significance was defined as  $P < 0.05$ .

**Results:** Median quantitative T<sub>2</sub> values were significantly lower for PCa in PZ (85 msec) and PCa in TZ (75 msec) compared to benign PZ (141 msec) or TZ (97 msec) ( $P < 0.001$ ). CD/CR between PCa and benign PZ (51.2/1.77), respectively TZ (19.8/1.29), differed significantly ( $P < 0.001$ ). The best T<sub>2</sub>-mapping threshold for PCa/csPCa detection was for TZ 81/86 msec ( $J = 0.929/1.0$ ), and for PZ 110 msec ( $J = 0.834/0.905$ ). Quantitative T<sub>2</sub> values of PCa did not correlate significantly with the ISUP grade ( $r_s = 0.186$ ;  $P = 0.226$ ), ADC value ( $r_s = 0.138$ ;  $P = 0.372$ ), or PI-RADS ( $r_s = 0.132$ ;  $P = 0.392$ ).

**Data Conclusion:** Quantitative T<sub>2</sub> values could differentiate PCa in TZ and PZ and might support standardization of mpMRI of the prostate. Different thresholds seem to apply for PZ and TZ lesions. However, in the present study quantitative T<sub>2</sub> values were not able to indicate PCa aggressiveness.

**Level of Evidence:** 2

**Technical Efficacy:** Stage 2

J. MAGN. RESON. IMAGING 2022;56:413–422.

Multiparametric magnetic resonance imaging (mpMRI) of the prostate shows excellent sensitivity in detecting clinically significant prostate cancer (csPCa).<sup>1</sup> Because of the dependence on reader experience, it has been an important goal to increase standardization of mpMRI examinations of the prostate.<sup>2</sup> Besides the development of the Prostate Imaging Reporting and Data System (PI-RADS, currently version 2.1),<sup>3,4</sup> another attempt to reduce inter-reader

View this article online at [wileyonlinelibrary.com](http://wileyonlinelibrary.com). DOI: 10.1002/jmri.28061

Received Oct 10, 2021, Accepted for publication Dec 22, 2021.

\*Address reprint requests to: L.S., Moorenstr. 5, D-40225 Dusseldorf, Germany. E-mail: [lars.schimmoller@med.uni-duesseldorf.de](mailto:lars.schimmoller@med.uni-duesseldorf.de)

From the <sup>1</sup>Department of Diagnostic and Interventional Radiology, University Dusseldorf, Medical Faculty, Dusseldorf, Germany; <sup>2</sup>MR Applications Predevelopment, Siemens Healthcare GmbH, Erlangen, Germany; <sup>3</sup>Department of Diagnostic and Interventional Radiology, University Hospital Jena, Jena, Germany; <sup>4</sup>Advanced Clinical Imaging Technology, Siemens Healthcare AG, Lausanne, Switzerland; <sup>5</sup>Department of Radiology, Lausanne University Hospital and University of Lausanne, Lausanne, Switzerland; <sup>6</sup>LTSS, École Polytechnique Fédérale de Lausanne, Lausanne, Switzerland; <sup>7</sup>SHS EMEA ST&BD SP PS&O, Siemens Healthcare GmbH, Eschborn, Germany; and <sup>8</sup>Department of Urology, University Dusseldorf, Medical Faculty, Dusseldorf, Germany

This is an open access article under the terms of the [Creative Commons Attribution-NonCommercial](https://creativecommons.org/licenses/by-nc/4.0/) License, which permits use, distribution and reproduction in any medium, provided the original work is properly cited and is not used for commercial purposes.

variability is to increasingly integrate quantitative parameters.  $T_2$  and  $T_2^*$  mapping already used in cardiac and cartilage imaging and have increasingly gained attention in prostate imaging to quantify  $T_2$  signal intensities.<sup>5–9</sup>

$T_2$ -weighted sequences enable the best available anatomic image characterization of the prostate, but standard  $T_2W$  signal intensities (SI) vary between sites because of varying sequence parameters, such as TR and TE, and radiofrequency inhomogeneity of the transmit and receive field and therefore cannot be used as a quantitative value. Instead,  $T_2$  mapping sequences focus on mapping the  $T_2$  relaxation time of the prostatic tissue. The relative percentages of stromal and glandular tissue, and therefore water components, vary between benign and cancerous prostatic tissue, which is the biophysical basis for  $T_2$  mapping.<sup>10</sup> Using a series of spin echo (SE) sequences, a signal decay curve can be acquired. Hereby, the  $T_2$  relaxation time of each voxel can be determined.<sup>11</sup>

$T_2$  mapping in prostate imaging has already been examined in several studies with most studies focusing on the peripheral zone (PZ).<sup>8,12–18</sup> However, a recent study was able to show significant results for PCa detection with quantitative  $T_2$  values in the transition zone (TZ) as well.<sup>15</sup> Furthermore, several studies showed evidence that quantitative  $T_2$  values correlate with PCa aggressiveness and therefore might enable the differentiation between significant and non-significant PCa (csPCa, nsPCa).<sup>15,19</sup> Recent literature concludes that further research is necessary regarding diagnostic accuracy of  $T_2$  mapping in PZ as well as TZ.<sup>8,9</sup>

Therefore, the aim of this study was to evaluate quantitative  $T_2$  values for PCa detection in PZ and TZ and to examine quantitative  $T_2$  values for the evaluation of cancer aggressiveness.

## Materials and Methods

### Study Design

This trial was approved by the institutional review board (Medical Faculty of the Heinrich-Heine-University Düsseldorf; Study-Nr: 5910R). All patients provided informed consent. Patients with elevated prostate-specific antigen (PSA) levels, mpMRI of the prostate including a  $T_2$ -mapping sequence, and subsequent transrectal ultrasound-guided biopsy (TRUS-GB) plus magnetic resonance imaging-guided biopsy (MRI/US fusion-guided) from 02/2019 to 12/2019 were included. Patients had to have no prior surgery or radiation treatment. This study includes only patients with histopathologically proven PCa.

### Study Objectives

The primary endpoint was the analysis of quantitative  $T_2$  values, contrast differences (CD) and contrast ratios (CR) between PCa and benign PZ, TZ, anterior fibromuscular stroma (AFS), and musculus obturatorius internus (MOI). Secondary objectives were analyses of correlation of quantitative  $T_2$  values with International Society of Urological Pathology (ISUP) grade, apparent diffusion coefficient (ADC) value, PI-RADS overall classification, and PI-RADS  $T_2$  single score. Furthermore, thresholds of quantitative  $T_2$  values for

**TABLE 1. MRI Parameter**

	$T_2$ Mapping	$T_2$ TSE	rs-EPI-DWI
Scanner	Siemens MAGNETOM Prisma 3 Tesla		
Coil	60-channel phased-array surface coil		
Orientation	Axial	Axial	Axial
TR (msec)	3900–9030	3990	4540
TE (msec)	10.8, 21.6, ..., 172.8 (16 echoes)	102	50
Slice thickness (mm)	3	3	3
Voxel size (mm <sup>3</sup> )	0.8 × 0.8 × 3	0.5 × 0.5 × 3	1.4 × 1.4 × 3
Field of view (mm <sup>2</sup> )	247 × 220	130 × 130	200 × 200
Matrix	320 × 270	256 × 256	140 × 140
Number of averages	1	3	1, 3
Number of slices	18–34	30	30
Acquisition Time (minutes:seconds)	3:26–7:58	5:19	6:38
<i>b</i> -values (seconds/mm <sup>2</sup> )	NA	NA	0, 1000
Calculated <i>b</i> -value	NA	NA	1800

TR = repetition time, TE = echo time.

differentiation between all PCa, csPCA, and benign tissue in PZ and TZ were analyzed.

### Imaging

MpMRI of the prostate was performed on a 3 T MRI scanner (MAGNETOM Prisma, Siemens Healthcare, Erlangen, Germany) with a phased-array surface coil in the supine position. The MRI protocol is in accordance with the recommendations of PI-RADS version 2.1.<sup>3,4,20</sup> It included T<sub>1</sub>WI (repetition time/echo time 870 msec/13 msec; slice thickness 5 mm; matrix 576 × 576; FOV 350 × 350 mm<sup>2</sup>) and T<sub>2</sub>WI turbo-spin-echo (TSE; 3990 msec/102 msec; 3 mm; 256 × 256; 130 × 130 mm<sup>2</sup>), dynamic contrast-enhanced (DCE; 3.87 msec/1.46 msec; 3 mm; 256 × 256; 200 × 200 mm<sup>2</sup>), diffusion-weighted imaging (DWI; 4540 msec/50 msec; 3 mm; 140 × 140; 200 × 200 mm<sup>2</sup>), and a prototype T<sub>2</sub>-mapping sequence (3900–9030 msec/16 echoes between 10.8–172.8 msec; 3 mm; 320 × 270; 247 × 220 mm<sup>2</sup>).<sup>21</sup> The detailed parameters of the T<sub>2</sub>-mapping, T<sub>2</sub> TSE, and DWI sequences are shown in Table 1. The readout segmented-DWI (rs-DWI; REadout Segmentation Of Long Variable Echo trains [RESOLVE]) was used for ADC value correlation.

### Biopsy and Histopathology

After mpMRI, all patients underwent targeted MRI/US fusion-guided and additional systematic (12-core) biopsy.<sup>22–24</sup> An experienced urologist performed all biopsies (5–10 years of experience in targeted prostate biopsy). All cancer-suspect regions (CSR) were marked with a three-dimensional region of interest (ROI) for biopsy targeting using DynaCAD Invivo (version 4, Philips Healthcare). Elastic MRI/US fusion was performed using UroNAV (Philips Healthcare). For targeted biopsy, two cores were obtained from each CSR. All biopsy cores were histopathologically evaluated in accordance with the recommendations of the ISUP by a pathologist. CsPCA was defined as ISUP grade ≥2.<sup>25</sup>

### Image Analysis

ROIs were defined by M.K. and L.S. (4 and 10 years of experience) in the T<sub>2</sub> map for the PCa index lesion, PZ, TZ, AFS, and MOI. PCa ROIs were selected according to the histopathologic report and corresponding lesion in ADC/DWI and T<sub>2</sub>W images. ROIs covered the center of the PCa lesion visible on MRI. In case a lesion involved more than one region, we decided on the main localization

**TABLE 2. Patient Characteristics**

Total number of patients with PCA included	44
Age (years), mean ± SD	67 ± 8.4
PSA (ng/mL), median (IQR)	7.9 (6.0–13)
Prostate volume (mL), median (IQR)	36 (29–49)
PI-RADS % (N)	
4	39 (17)
5	61 (27)
ISUP Grade Group % (N)	
1	41 (18)
2	23 (10)
3	6.8 (3)
4	25 (11)
5	4.5 (2)
PCa Localization % (N)	
PZ	68 (30)
TZ	20 (9)
AFS	11 (5)
Maximum diameter of PCa index lesion (mm), median (IQR)	16 (12–20)

SD = standard deviation; PSA = prostate-specific antigen; IQR = interquartile range; PCa = prostate carcinoma; ISUP = International Society of Urological Pathology; PZ = peripheral zone; TZ = transition zone; AFS = anterior fibromuscular stroma.

based on the main tumor volume. For PZ, TZ, AFS, and MOI, ROIs were drawn as large as possible around the tissue. ROIs were copied in each sequence to ensure matching sizes. An example of the

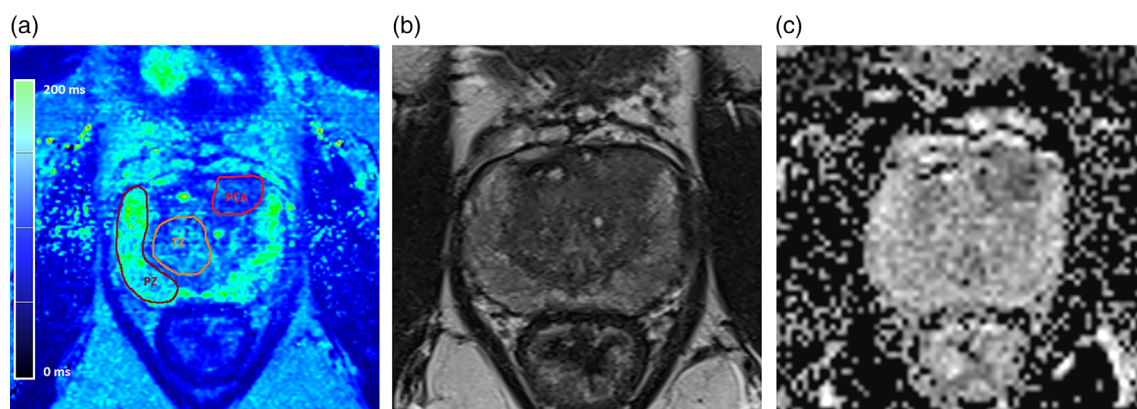


**FIGURE 1:** ROI measurements of benign tissue in the peripheral zone (PZ; purple ROI) and transition zone (TZ; orange ROI), and PCa (red ROI). Quantitative T<sub>2</sub> map (a), T<sub>2</sub> TSE (b), and calculated ADC map of rs-DWI (c). On radical prostatectomy (RPE), an ISUP grade 5 PCa was confirmed.

**TABLE 3. Quantitative T<sub>2</sub> Values**

	ROI Size <sup>a</sup> , Median (IQR)	T <sub>2</sub> Value <sup>b</sup> , Median (IQR)	ADC Value, Median (IQR)	PI-RADS, Median (IQR)
All (N = 44)				
PCa	0.66 (0.46–0.87)	79.9 (75.2–88.2)	869 (774–968)	5 (4–5)
PZ	1.35 (1.08–1.74)	136 (117–161)		
TZ	1.31 (1.01–1.57)	102 (89.2–115)		
AFS	0.78 (0.66–1.13)	87.5 (79.4–98.0)		
MOI	0.95 (0.7–1.31)	47.3 (43.8–52.6)		
PCa in PZ (N = 30)				
PCa	0.64 (0.44–0.84)	84.6 (79.1–96.2)	898 (779–969)	5 (4–5)
PZ	1.32 (1.08–1.73)	141 (119–171)		
PCa in TZ (N = 14)				
PCa	0.66 (0.53–0.92)	74.8 (70.4–77.7)	835 (780–877)	5 (4–5)
TZ	1.32 (1.0–1.46)	96.8 (90.9–113)		
ISUP 1 (N = 18)				
PCa	0.59 (0.46–0.92)	76.5 (71.5–87.3)	898 (839–987)	4 (4–5)
PZ	1.56 (1.14–1.94)	129 (109–159)		
TZ	1.4 (0.97–1.58)	102 (87.9–109)		
AFS	1.03 (0.74–1.25)	87.1 (79.5–92.4)		
MOI	1.2 (0.72–1.55)	48.8 (44.9–54.7)		
ISUP ≥2 (N = 26)				
PCa	0.70 (0.45–0.92)	80.4 (77.4–90.3)	846 (708–918)	5 (4–5)
PZ	1.24 (1.06–1.65)	136 (119–161)		
TZ	1.24 (1.02–1.55)	102 (90.9–115)		
AFS	0.72 (0.63–0.86)	89.9 (71.5–105)		
MOI	0.88 (0.72–1.28)	46.9 (43.5–51.1)		
ISUP ≥3 (N = 16)				
PCa	0.74 (0.58–1.12)	84.6 (79.6–92.2)	822 (688–913)	5 (5–5)
PZ	1.28 (1.07–1.69)	135 (117–167)		
TZ	1.29 (1.14–1.68)	103 (91.1–116)		
AFS	0.72 (0.65–0.78)	105 (85.8–106)		
MOI	0.84 (0.77–1.21)	48.0 (45.2–50.4)		

ROI = region of interest; IQR = interquartile range; ADC = apparent diffusion coefficient; PCa = prostate carcinoma; PZ = peripheral zone; TZ = transition zone; AFS = anterior fibromuscular stroma; MOI = musculus obturatorius internus; ISUP = International Society of Urological Pathology.

<sup>a</sup>In square centimeters.

<sup>b</sup>In milliseconds.

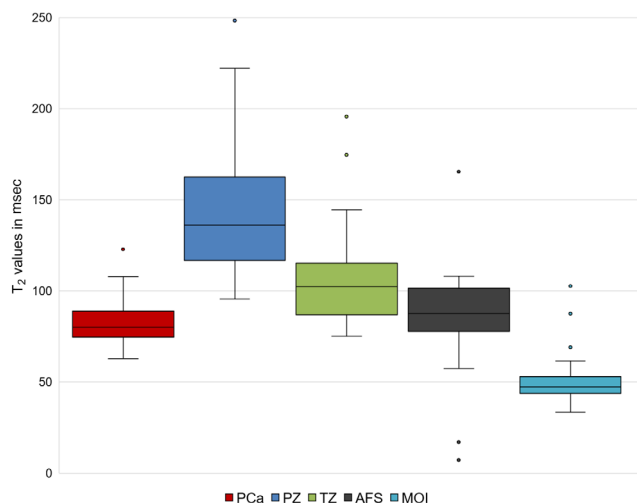


**FIGURE 2:** Boxplot of quantitative T<sub>2</sub> values in PCa, PZ, TZ, AFS, and MOI.

selected ROIs is shown in Fig. 1. CD was calculated as difference and CR as ratio between quantitative T<sub>2</sub> values in PZ, respectively TZ, and PCa in the anatomic zone. Quantitative T<sub>2</sub> values of the PCa index lesion were compared with the respective ISUP grade.

### Statistical Analysis

Data were presented as mean  $\pm$  standard deviation or median and interquartile range (IQR). SPSS (version 2019) was used for analysis of non-parametric data with Mann–Whitney test and Spearman ( $r_s$ ) for correlation analysis. Statistical significance was defined as  $P$ -value  $< 0.05$ . Cut-off values were determined using Youden's index (J) and Area under the curve (AUC). Boxplots were created using Microsoft Excel (version 2019).

## Results

### Patient Population

Forty-four male patients ( $67 \pm 8.4$  years) were included in this study. Details of patient population are shown in

Table 2. Time interval between mpMRI and biopsy was 20 days median (IQR 19–26 days).

### Analysis of PCa Detection

Analysis showed that PCa T<sub>2</sub> values (80 msec, IQR 75–88 msec; ROI size median 0.66 cm<sup>2</sup>, IQR 0.46–0.87 cm<sup>2</sup>) were significantly lower than benign PZ (136 msec, IQR 117–161 msec; ROI size median 1.35 cm<sup>2</sup>, IQR 1.08–1.74 cm<sup>2</sup>) and/or TZ (102 msec, IQR 89–115 msec; ROI size median 1.31 cm<sup>2</sup>, IQR 1.01–1.57 cm<sup>2</sup>) ( $P < 0.001$ ). T<sub>2</sub> values of MOI compared to PCa were significantly lower (48 msec, IQR 44–53 msec; ROI size median 0.95 cm<sup>2</sup>, IQR 0.7–1.3 cm<sup>2</sup>) ( $P < 0.001$ ). No significant differences were detected between PCa and AFS (88 msec, IQR 79–98 msec; ROI size median 0.78 cm<sup>2</sup>, IQR 0.66–1.13 cm<sup>2</sup>) ( $P = 0.984$ ). Quantitative T<sub>2</sub> values analysis is shown in Table 3 and Fig. 2.

The T<sub>2</sub> values of PCa in PZ (85 msec, IQR 79–96 msec; ROI size median 1.32 cm<sup>2</sup>, IQR 1.08–1.73 cm<sup>2</sup>) and PCa in TZ (75 msec, IQR 70–78 msec; ROI size median 1.32 cm<sup>2</sup>, IQR 1.00–1.46 cm<sup>2</sup>) showed significantly lower quantitative T<sub>2</sub> values compared to the respectively benign PZ (141 msec, IQR 119–171 msec) and TZ (97 msec, IQR 91–113 msec) ( $P < 0.001$ ). CD/CR for PCa in PZ (51.2; IQR 31.7–83.2) as well as PCa in TZ (19.8; IQR 7.68–30.3) and the benign tissue were significantly different ( $P < 0.001$ ). CD/CR values are shown in Table 4, pointing out the highest CD/CR between PCa and PZ. Figure 3 shows boxplots for PCa in PZ and TZ.

Youden's index (J) showed that the best cut-off T<sub>2</sub> value was 92 msec (specificity 86%, sensitivity 80%) for PCa and 99 msec (specificity 79%, sensitivity 89%) for csPCa with an AUC value of 0.90, respectively (Fig. 4). For PCa/csPCa in TZ 81/86 msec (AUC 0.99) and for PCa/csPCa in PZ of 110/110 msec (AUC 0.98) (Table 5).

**TABLE 4.** Contrast Difference (CD) and Contrast Ratio (CR) of Quantitative T<sub>2</sub> Values

	CD, Median (IQR)	CR, Mean $\pm$ SD
All (N = 44)		
PZ and PCa	51.2 (31.7 to 83.2)	1.77 $\pm$ 0.49
TZ and PCa	19.8 (7.68 to 30.3)	1.29 $\pm$ 0.33
AFS and PCa	5.3 (–3.1 to 16.2)	1.14 $\pm$ 0.34
MOI and PCa	–31.3 (–40.4 to –23.6)	0.61 $\pm$ 0.12
PCA in PZ and TZ		
PZ and PCa in PZ (N = 30)	51.1 (29.2–84.7)	1.75 $\pm$ 0.53
TZ and PCa in TZ (N = 14)	24.5 (18.0–35.8)	1.35 $\pm$ 0.14

PCa = prostate carcinoma; PZ = peripheral zone; TZ = transition zone; AFS = anterior fibromuscular stroma; MOI = musculus obturatorius internus.



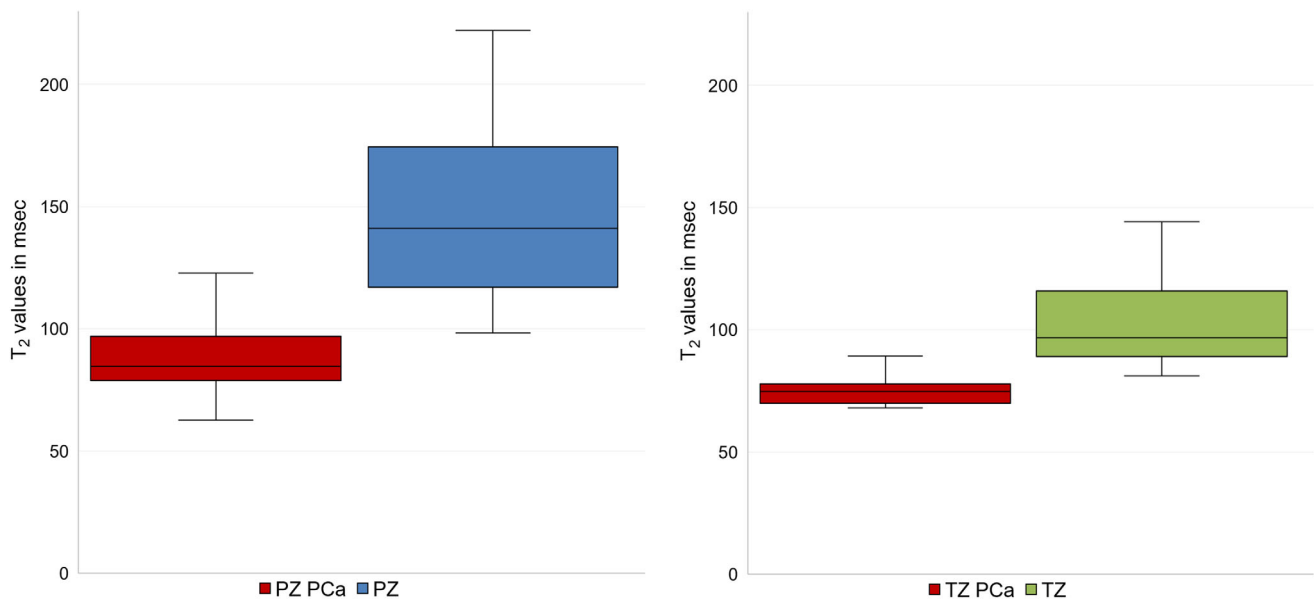


FIGURE 3: Boxplot of quantitative  $T_2$  values separate for PZ PCa and TZ PCa.

### Analysis of PCa Classification

$T_2$  values did not significantly correlate with the ISUP grade ( $P = 0.226$ ). Figure 5 shows boxplots for all ISUP grades and demonstrates a substantial overlap for the quantitative  $T_2$  values of all groups. Quantitative  $T_2$  values of PCa/csPCa also did not significantly correlate with ADC ( $P = 0.372/0.534$ ). Moreover, there was no significant correlation between quantitative  $T_2$  values of PCa/csPCa and PI-RADS ( $P = 0.392/0.534$ ) and  $T_2$  score ( $P = 0.371/0.951$ ) (Table 6).

### Discussion

The results show that quantitative  $T_2$  values were significantly lower in both PZ and TZ compared to benign tissue and therefore enabled the detection of PCa. Quantitative  $T_2$  values may be a valuable addition to the standard mpMRI protocol striving to increase standardization. However, different thresholds seem to be required for PZ and TZ. Tumor grading seems limited with quantitative  $T_2$  values.

Current studies show that MR plays an important role in PCa grading, particularly by combining quantitative and qualitative parameters.<sup>3,26</sup> A large meta-analysis by Meyer et al. including 26 studies has recently again confirmed that ADC values correlate with the Gleason score.<sup>27</sup>  $T_2$  and  $T_2^*$  mapping was analyzed in several studies, specifically whether it is possible to differentiate cancer aggressiveness.<sup>15,18,19</sup> Mai et al found that low quantitative  $T_2$  values were associated with higher PCa aggressiveness.<sup>15</sup> However, these results showed no significant correlation between quantitative  $T_2$  values of PCa and the ISUP grade. Reasons for that might be different lesion rendering, different ISUP distribution of the patient collective and/or the small sample size for each ISUP

grade group. Walker et al. concluded that this is especially due small sample sizes and retrospective analysis. Hence, further studies are necessary on this topic.<sup>9</sup>

It is important to evaluate the anatomic zones of the prostate separately because of different  $T_2$  relaxation times. This study confirmed that quantitative  $T_2$  values for benign tissue in TZ compared to PZ are significantly lower. The majority of  $T_2$  mapping studies focusing the PZ with the aim to establish a threshold for differentiation between benign tissue and PCa.<sup>8,12–18</sup> Yamauchi et al. demonstrated a specificity of 92% and specificity of 99% for a threshold of 99 msec.<sup>16</sup> This study showed significantly lower quantitative  $T_2$  values for PCa in PZ compared to benign tissue and a higher CR in PZ. Moreover, these results are comparable regarding specificity and sensitivity using a higher threshold. However, prostatitis may lead to masked or missed detection of PCa in PZ on  $T_2$ W images.<sup>28</sup> Cases with prostatitis may lead to a PI-RADS 3 classification and have not been included in the study. Therefore, further studies are necessary in order to discover whether quantitative  $T_2$  values can solve this predicament.<sup>8</sup>

Current literature reports a significantly lower quantitative  $T_2$  relaxation time in TZ compared to PZ, which can be caused by for example, stromal hyperplasia.<sup>8,29</sup> Most of the previous studies focused on PZ PCa or showed limited results for TZ PCa detection.<sup>8,9,12–18</sup> However, Mai et al showed significant differences between benign tissue and PCa in TZ.<sup>15</sup> These results are comparable to the present study. The present data even suggest a substantially lower threshold that leads to an even higher specificity. Besides stromal hyperplasia<sup>8,29</sup> further reasons for different  $T_2$  relaxation times for PCa in PZ and TZ could include different ISUP grading or different tumor cell type. These hypotheses need to be further evaluated in larger

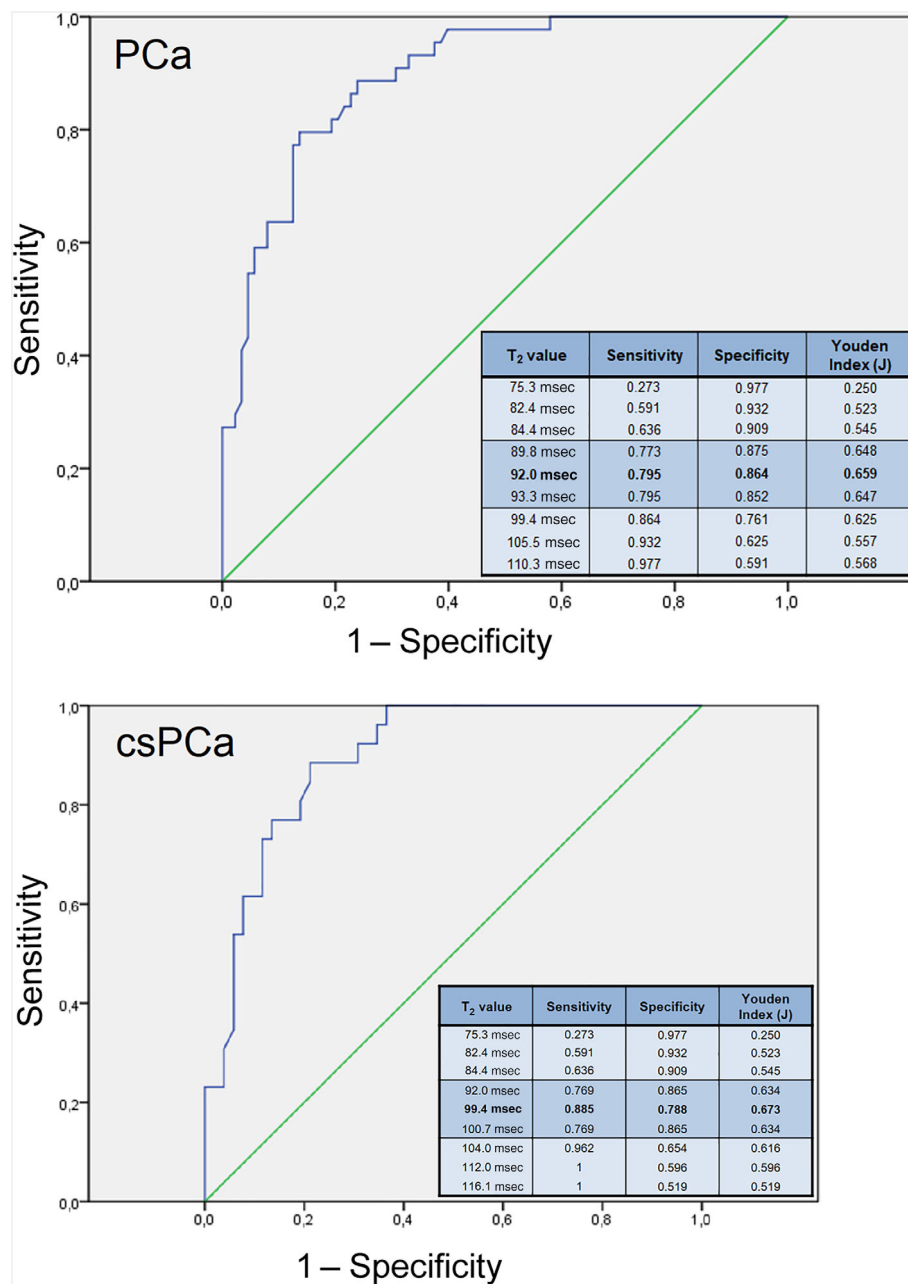


FIGURE 4: ROC analysis for PCa/csPca detection by quantitative T<sub>2</sub> value.

studies. Nevertheless, quantitative T<sub>2</sub> mapping is supposed to be used in addition to the standard mpMRI protocol according to the PI-RADS recommendation.<sup>3,4,30</sup>

There were no significant differences of quantitative T<sub>2</sub> values between PCa and AFS, which might underline the benefit of DWI and/or DCE to detect anterior PCa. Furthermore, we could show that T<sub>2</sub> values of MOI are significantly lower compared to PCa. Therefore, MOI signal intensity might be used as a reference signal intensity.

Establishing a reliable cut-off for T<sub>2</sub> values has been a challenging task. Current literature has reported thresholds for quantitative T<sub>2</sub> values in a range between 99 msec<sup>16</sup> to 134 msec<sup>15</sup> in PZ. The presence of (stromal) hyperplasia

and/or prostatitis next to a possible variability of T<sub>2</sub> values depending on the scanner vendor and sequence type makes it difficult to establish generally usable cut-off values.<sup>13,28</sup> Nonetheless, Hoang et al. concluded that T<sub>2</sub> values were robust to scanner and vendor changes.<sup>13</sup>

#### Limitations

Limitations of this study include the single center and single scanner/field strength design with a small sample size. Furthermore, signs of hyperplasia and prostatitis may have an impact of the ability to differentiate PCa from benign tissue using quantitative T<sub>2</sub> values. However, since almost all patients have some degree of benign hyperplasia and often

**TABLE 5. Sensitivity, Specificity, and Youden Index for PCa/csPCa Detection in PZ and TZ**

	T <sub>2</sub> Value	Sensitivity	Specificity	Youden Index (J)
PCa in TZ	73.9 msec	0.429	1	0.429
	77.6 msec	0.714	1	0.714
	79.3 msec	0.857	1	0.857
	<b>80.9 msec</b>	<b>0.929</b>	<b>1</b>	<b>0.929</b>
	81.6 msec	0.929	0.929	0.858
	87.3 msec	0.929	0.786	0.715
	94.3 msec	1	0.571	0.571
csPCa in TZ	71.7 msec	0.4	1	0.4
	75.7 msec	0.6	1	0.6
	79.3 msec	0.8	1	0.8
	<b>85.5 msec</b>	<b>1</b>	<b>1</b>	<b>1</b>
	91.6 msec	1	0.8	0.8
	93.3 msec	1	0.6	0.6
	104.8 msec	1	0.4	0.4
PCa in PZ	82.9 msec	0.467	1	0.467
	93.3 msec	0.7	1	0.700
	106.7 msec	0.933	0.900	0.833
	<b>109.9 msec</b>	<b>0.967</b>	<b>0.867</b>	<b>0.834</b>
	112.0 msec	0.967	0.833	0.800
	120.0 msec	0.967	0.733	0.700
	134.8 msec	1	0.567	0.567
csPCa in PZ	82.9 msec	0.476	1	0.476
	95.9 msec	0.762	1	0.762
	106.0 msec	0.952	0.905	0.857
	<b>109.9 msec</b>	<b>1</b>	<b>0.905</b>	<b>0.905</b>
	112.0 msec	1	0.857	0.857
	121.5	1	0.667	0.667
	134.8	1	0.524	0.524

PCa = prostate carcinoma; csPCa = clinically significant prostate carcinoma; PZ = peripheral zone; TZ = transition zone; bold = highest Youden Index (J).

additional signs of prostatitis, exact histological localization of the PCa allowed placing the ROI in the PCa lesion correlated in all available sequences and other ROIs in regions that showed benign histological results. Thus, overlaying hyperplasia and prostatitis may have influence on the signal, because of their ubiquitous presence, these effects counterbalanced themselves and differentiation of PCa and benign tissue was

still possible within the same patients. In addition, it is very difficult to confirm how much calcification in the TZ affects the T<sub>2</sub> relaxation time. No patients without PCa were included. Also, a study control group analysis is warranted. Moreover, since the exact size of the lesion was not confirmed with the surgical specimen, the degree of agreement between PCa and ROI could not be confirmed. Due to these



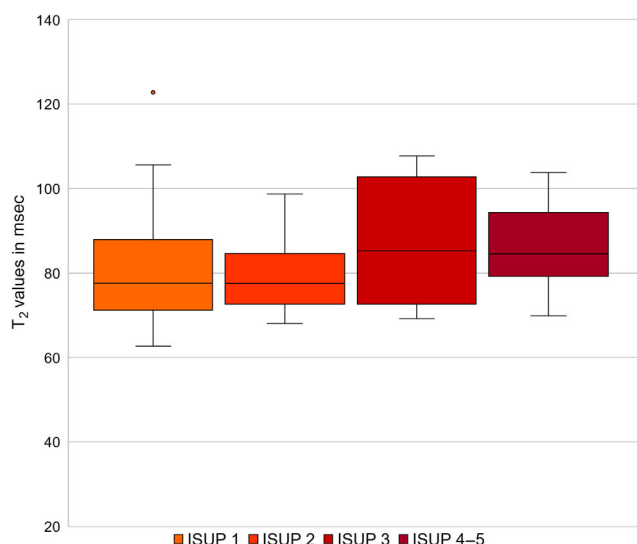


**FIGURE 5:** Boxplot of quantitative T<sub>2</sub> values for different ISUP grades.

**TABLE 6.** Correlation of T<sub>2</sub> Values, ISUP, ADC, PI-RADS, and T<sub>2</sub> Score

	<i>r<sub>s</sub></i>	<i>P</i> -Value
Correlation With T <sub>2</sub> Value of PCa		
ADC	0.138	0.372
ISUP	0.186	0.226
PI-RADS	0.132	0.392
T <sub>2</sub> score	0.138	0.371
Correlation With T <sub>2</sub> Value of csPCa		
ADC	0.128	0.534
PI-RADS	0.128	0.534
T <sub>2</sub> score	0.013	0.951

PCa = prostate carcinoma; csPCa = clinically significant prostate carcinoma; ADC = apparent diffusion coefficient; ISUP = International Society of Urological Pathology; PI-RADS = Prostate Imaging Reporting and Data System.

limitations further larger (multi-center) studies are needed to approach the problem of determining a threshold.

## Conclusion

Quantitative T<sub>2</sub> values seem promising for standardization of PCa detection on T<sub>2</sub> images. Different thresholds seem needed to apply for PCa detection in PZ and TZ. PCa detection in AFS was limited with only the use of T<sub>2</sub> images and the present study found no significantly different quantitative T<sub>2</sub> values between non-significant and significant PCa. This

underlines the current recommended multiparametric setting for PCa detection with MRI.

## Acknowledgment

Open access funding enabled and organized by Projekt DEAL.

## Conflict of Interest

Franiel Tobias: Grant support: Zentrales Innovationsprogramm Mittelstand des Bundesministeriums für Wirtschaft und Energie (ZF4816001BA9); Institutional research cooperation: Siemens Healthineers; Honoraria/speaker/travel support: Bayer AG, Saegeling Medizintechnik GmbH, Medac GmbH; Royalties: Georg Thieme Verlag; Advisory Board: Bayer AG.

## References

- Ahmed HU, El-Shater Bosaily A, Brown LC, et al. Diagnostic accuracy of multi-parametric MRI and TRUS biopsy in prostate cancer (PROMIS): A paired validating confirmatory study. *Lancet* 2017;389:815. [https://doi.org/10.1016/S0140-6736\(16\)32401-1](https://doi.org/10.1016/S0140-6736(16)32401-1).
- Ruprecht O, Weisser P, Bodelle B, et al. MRI of the prostate: Inter-observer agreement compared with histopathologic outcome after radical prostatectomy. *Eur J Radiol* 2012;81:456. <https://doi.org/10.1016/j.ejrad.2010.12.076>.
- Weinreb JC, Barentsz JO, Choyke PL, et al. PI-RADS prostate imaging-reporting and data system: 2015, version 2. *Eur Urol* 2016;69:16. <https://doi.org/10.1016/j.eururo.2015.08.052>.
- Turkbey B, Rosenkrantz AB, Haider MA, et al. Prostate imaging reporting and data system version 2.1: 2019 Update of prostate imaging reporting and data system version 2. *Eur Urol* 2019;76(3):340–351. <https://doi.org/10.1016/j.eururo.2019.02.033>.
- Wiesmueller M, Wuest W, Heiss R, et al. Cardiac T2 mapping: Robustness and homogeneity of standardized in-line analysis. *J Cardiovasc Magn Reson* 2020;22:39. <https://doi.org/10.1186/s12968-020-00619-x>.
- Roux M, Hilbert T, Hussami M, Becce F, Kober T, Omoumi P. MRI T2 mapping of the knee providing synthetic morphologic images: Comparison to conventional turbo spin-echo MRI. *Radiology* 2019;293(3):620–630.
- Bittersohl B, Miese FR, Hosalkar HS, et al. T<sub>2</sub>\* mapping of acetabular and femoral hip joint cartilage at 3 T: A prospective controlled study. *Invest Radiol* 2012;47:392. <https://doi.org/10.1097/RLI.0b013e3182518d57>.
- Lee CH. Quantitative T2-mapping using MRI for detection of prostate malignancy: A systematic review of the literature. *Acta Radiol* 2019; 60(9):1181. <https://doi.org/10.1177/0284185118820058>.
- Walker SM, Fernandez M, Turkbey B. Advances in prostate magnetic resonance imaging. *Magn Reson Imaging Clin N Am* 2020;28:407. <https://doi.org/10.1016/j.mric.2020.03.006>.
- Nguyen K, Sarkar A, Jain AK. Prostate cancer grading: Use of graph cut and spatial arrangement of nuclei. *IEEE Trans Med Imaging* 2014;33: 2254. <https://doi.org/10.1109/TMI.2014.2336883>.
- Noth U, Shrestha M, Schure JR, et al. Quantitative in vivo T2 mapping using fast spin echo techniques—A linear correction procedure. *Neuroimage* 2017;157:476. <https://doi.org/10.1016/j.neuroimage.2017.06.017>.
- Metzger GJ, Kalavagunta C, Spilseth B, et al. Detection of prostate cancer: Quantitative multiparametric MR imaging models developed using registered correlative histopathology. *Radiology* 2016;279:805. <https://doi.org/10.1148/radiol.2015151089>.

13. Hoang DA, Souchon R, Melodelima C, et al. Characterization of prostate cancer using T2 mapping at 3T: A multi-scanner study. *Diagn Interv Imaging* 2015;96:365. <https://doi.org/10.1016/j.diii.2014.11.016>.
14. Hoang DA, Melodelima C, Souchon R, et al. Quantitative analysis of prostate multiparametric MR images for detection of aggressive prostate cancer in the peripheral zone: A multiple imager study. *Radiology* 2016;280:117. <https://doi.org/10.1148/radiol.2016151406>.
15. Mai J, Abubrig M, Lehmann T, et al. T2 mapping in prostate cancer. *Invest Radiol* 2019;54:146. <https://doi.org/10.1097/RLI.0000000000000520>.
16. Yamauchi FI, Penzkofer T, Fedorov A, et al. Prostate cancer discrimination in the peripheral zone with a reduced field-of-view T (2)-mapping MRI sequence. *Magn Reson Imaging* 2015;33:525. <https://doi.org/10.1016/j.mri.2015.02.006>.
17. Chatterjee A, Devaraj A, Mathew M, et al. Performance of T2 maps in the detection of prostate cancer. *Acad Radiol* 2019;26:15. <https://doi.org/10.1016/j.acra.2018.04.005>.
18. Wu LM, Yao QY, Zhu J, et al. T<sub>2</sub>\* mapping combined with conventional T2-weighted image for prostate cancer detection at 3.0T MRI: A multi-observer study. *Acta Radiol* 2017;58:114. <https://doi.org/10.1177/0284185116633916>.
19. Wu LM, Chen XX, Xuan HQ, et al. Feasibility and preliminary experience of quantitative T<sub>2</sub>\* mapping at 3.0 T for detection and assessment of aggressiveness of prostate cancer. *Acad Radiol* 2014;21:1020. <https://doi.org/10.1016/j.acra.2014.04.007>.
20. Quentin M, Schimmoller L, Arsov C, et al. Increased signal intensity of prostate lesions on high b-value diffusion-weighted images as a predictive sign of malignancy. *Eur Radiol* 2014;24:209. <https://doi.org/10.1007/s00330-013-2999-3>.
21. Hilbert T, Sumpf TJ, Weiland E, et al. Accelerated T2 mapping combining parallel MRI and model-based reconstruction: GRAPPATINI. *J Magn Reson Imaging* 2018;48:359-368.
22. Quentin M, Blondin D, Arsov C, et al. Prospective evaluation of magnetic resonance imaging guided in-bore prostate biopsy versus systematic transrectal ultrasound guided prostate biopsy in biopsy naive men with elevated prostate specific antigen. *J Urol* 2014;192:1374. <https://doi.org/10.1016/j.juro.2014.05.090>.
23. Arsov C, Becker N, Rabenalt R, et al. The use of targeted MR-guided prostate biopsy reduces the risk of Gleason upgrading on radical prostatectomy. *J Cancer Res Clin Oncol* 2015;141:2061. <https://doi.org/10.1007/s00432-015-1991-5>.
24. Arsov C, Rabenalt R, Blondin D, et al. Prospective randomized trial comparing magnetic resonance imaging (MRI)-guided in-bore biopsy to MRI-ultrasound fusion and transrectal ultrasound-guided prostate biopsy in patients with prior negative biopsies. *Eur Urol* 2015;68:713. <https://doi.org/10.1016/j.eururo.2015.06.008>.
25. Epstein JI, Egevad L, Amin MB, et al. The 2014 International Society of Urological Pathology (ISUP) consensus conference on Gleason grading of prostatic carcinoma: Definition of grading patterns and proposal for a new grading system. *Am J Surg Pathol* 2016;40:244. <https://doi.org/10.1097/PAS.0000000000000530>.
26. Boschheidgen M, Schimmöller L, Arsov C, et al. MRI grading for the prediction of prostate cancer aggressiveness. *Eur Radiol* 2021. <https://doi.org/10.1007/s00330-021-08332-8>.
27. Meyer HJ, Wienke A, Surov A. Discrimination between clinical significant and insignificant prostate cancer with apparent diffusion coefficient—A systematic review and meta analysis. *BMC Cancer* 2020;20:482. <https://doi.org/10.1186/s12885-020-06942-x>.
28. Kitzing YX, Prando A, Varol C, et al. Benign conditions that mimic prostate carcinoma: MR imaging features with histopathologic correlation. *Radiographics* 2016;36(1):162. <https://doi.org/10.1148/rg.2016150030>.
29. Lim KB. Epidemiology of clinical benign prostatic hyperplasia. *Asian J Urol* 2017;4:148. <https://doi.org/10.1016/j.ajur.2017.06.004>.
30. Panebianco V, Giganti F, Kitzing YX, et al. An update of pitfalls in prostate mpMRI: A practical approach through the lens of PI-RADS v. 2 guidelines. *Insights Imaging* 2018;9:87. <https://doi.org/10.1007/s13244-017-0578-x>.